Supplementary Table 1. Structure parameters of NH_3He

Space group	Pressure (GPa)	Stoichiometry per Unit cell	Lattice Parameters (Å, °)			Atomic coordinates (Fractional coordinates)				multiplicity
$P2_12_12_1$	600	$N_4H_{12}He_4$	*a*=3.467	*b*=2.291	*c*=4.219	N	0.3657	0.0067	0.0763	4
			$\alpha = 90$	$\beta = 90$	$\gamma = 90$	H1	0.3846	0.3191	0.4690	4
						H2	0.1067	0.5857	0.5636	4
						H3	0.7180	0.4482	0.2052	4
						He	0.5965	0.0185	0.7273	4

Supplementary Table 2. Structure parameters of $(H_2O)_2He$

Space group	Pressure (GPa)	Stoichiometry per Unit cell	Lattice Parameters (Å, °)			Atomic coordinates (Fractional coordinates)				multiplicity
$Ibam$	600	$H_{16}O_8He_4$	*a*=3.995	*b*=3.936	*c*=3.290	H1	0.7445	0.5820	0.0000	8
			$\alpha = 90$	$\beta = 90$	$\gamma = 90$	H2	0.0000	0.6738	0.2500	8
						O	0.6630	0.8295	0.0000	8
						He	0.0000	0.0000	0.2500	4

Supplementary Table 3. Structure parameters of NH_3

Space group	Pressure (GPa)	Stoichiometry per unit cell	Lattice Parameters (Å, °)			Atomic coordinates (Fractional coordinates)				Multiplicity
$P2_13$	0.1	N_4H_{12}	*a*=5.084	*b*=5.084	*c*=5.084	N	0.4506	0.4506	0.4506	4
			$\alpha = 90$	$\beta = 90$	$\gamma = 90$	H	0.8495	-0.0221	0.3897	12
$P2_12_12_1$	50	N_4H_{12}	*a*=2.740	*b*=4.522	*c*=4.757	N	0.0145	-0.0042	0.0910	4
			$\alpha = 90$	$\beta = 90$	$\gamma = 90$	H1	0.0316	0.1961	0.1919	4
						H2	0.8862	0.0294	0.8935	4
						H3	0.3629	-0.0768	0.0719	4
$Pma2$	200		*a*=6.958	*b*=2.372	*c*=2.371	N1	0.0000	0.0000	0.2181	2
			$\alpha = 90$	$\beta = 90$	$\gamma = 90$	N2	0.2500	0.5024	0.7093	2
						H1	0.5821	0.7563	-0.0289	4
						H2	0.4118	0.7505	0.4640	4
						H3	0.2500	0.0827	0.6394	2
						H4	0.2500	0.5731	0.1295	2
$P2_1/m$	350	N_4H_{12}	*a*=2.266	*b*=3.684	*c*=3.892	N1	0.5185	0.2500	0.6693	2
			$\alpha = 90$	$\beta = 90.5$	$\gamma = 90$	N2	-0.0687	0.2500	0.1714	2
						H1	0.3034	0.2500	0.8826	2
						H2	0.7885	0.4597	0.6763	4
						H3	0.5078	0.2500	0.1965	2
						H4	0.0000	0.0000	0.0000	2
						H5	0.2178	0.2500	0.4795	2
$Pnma$	600	N_4H_{12}	*a*=3.611	*b*=3.515	*c*=2.102	N1	0.1368	0.2500	0.5737	4
			$\alpha = 90$	$\beta = 90$	$\gamma = 90$	H1	0.3450	0.5411	0.3690	8
						H2	0.4127	0.2500	0.1876	4

Supplementary Table 4. Structure parameters of H_2O

Space group	Pressure	Stoichiometry	Lattice Parameters			Atomic coordinates				multiplicity
	(GPa)	per unit cell	(Å, °)			(Fractional coordinates)				
$Cmc2_1$	0.1	$H_{16}O_8$	*a*=4.337	*b*=7.519	*c*=7.081	H1	0.6858	0.2317	0.0172	8
			$\alpha = 90$	$\beta = 90$	$\gamma = 90$	H2	0.0000	0.3348	0.7991	4
						H3	0.0000	0.4603	-0.0160	4
						O1	0.0000	0.3328	-0.0588	4
						O2	0.0000	0.6661	0.0660	4
$Pn\bar{3}m$	300	H_4O_2	*a*=2.443	*b*=2.443	*c*=2.443	H	0.2500	0.2500	0.2500	4
			$\alpha = 90$	$\beta = 90$	$\gamma = 90$	O	0.0000	0.0000	0.0000	2
$Pbcm$	600	H_8O_4	*a*=2.018	*b*=3.474	*c*=3.309	H1	-0.0022	0.1651	0.2500	4
			$\alpha = 90$	$\beta = 90$	$\gamma = 90$	H2	0.5000	0.0000	0.0000	4
						O	0.2571	0.4084	0.2500	4

Supplementary Note 1

In Supplementary Fig. 1, we show the DOS and PDOS for He-NH_3 and He-H_2O system. In Supplementary Fig. 1a and c, we show the DOS of $(H_2O)_2He$ and H_2O under pressure of 400 GPa. The He insertion makes the H_2O band gap slightly increases from 9.25 eV to 10.06 eV. From the He 1s and 2p orbital, there is no obvious hybridization with other orbitals, which suggests He forms no bonds with its neighbor ions. We can also see the He insertion close the small gap between the O 2s and 2p orbital, which means although He doesn't form any bonds, its existence changes other elements' electronic structure. In the case of NH_3He (Supplementary Fig. 1b) and NH_3 (Supplementary Fig. 1d), the NH_3He has a slight larger band gap that the one of NH_3 under pressure of 400 GPa. The bandgap in NH_3He is 4.06 eV while 3.01 eV in NH_3. Also, the N s and p orbital hybridization property is changed by He insertion from the comparison the PDOS of NH_3He and NH_3.

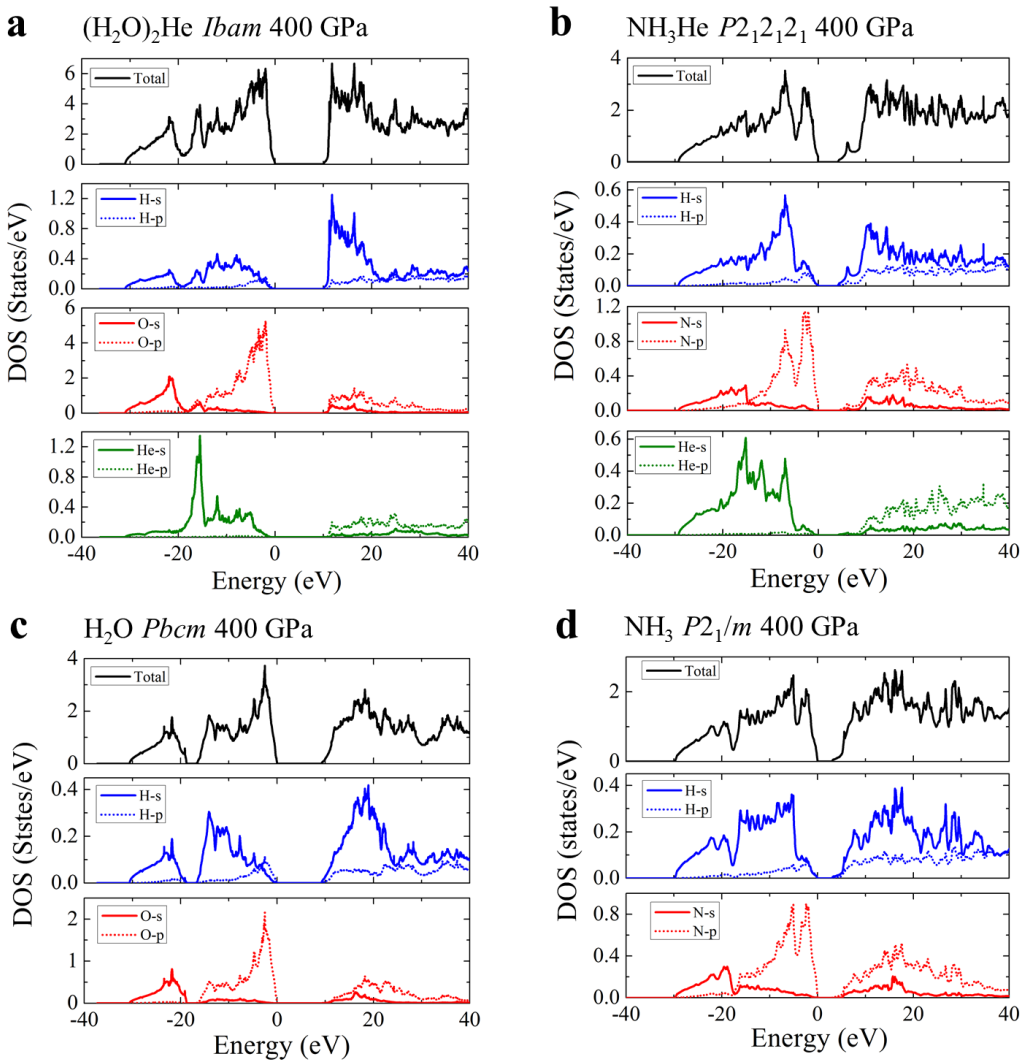

Supplementary Figure 1. The density of states (DOS) of H_2O+He and NH_3+He systems under 400 GPa. (a) $(H_2O)_2He$ with the space group of *Ibam*. (b)NH_3He with the space group $P2_12_12_1$. (c) H_2O with the space group of *Pbcm* (d) NH_3 with the space group $P2_1/m$.

Supplementary Note 2

Using the LMTO method, we calculate the Integrated Crystal Orbital Hamilton Population[1] (ICOHP) of He and its neighbor ions to investigate the possible bond strength of He. The results are shown in Supplementary Table 5 and Supplementary Table 6. The ICOHP for the pair of He and its neighboring N, O, H atoms are calculated under 400 GPa and 500 GPa for $(H_2O)_2He$ and NH_3He. In the case of H_2O+He, He-O ICOHP are 0.007 eV/pair and 0.054 eV/pair at 400 GPa and 500 GPa respectively, which shows a negligible bonding. He-H ICOHP values are small but not negligible. H ions have 2 equivalent position in the *Ibam* space group structure of $(H_2O)_2He$, which are denote as H1 and H2, see Supplementary Table 2. At 400 GPa, The ICOHP of He-H1 and He-H2 are 0.434 and 0.225 eV/pair. At 600 GPa, the corresponding ICOHP are 0.116 and 0.148 eV/pair. In the case of NH_3+He, He-N ICOHP are 0.126 and 0.140 eV/pair at 400 GPa and 500 GPa. He and its neighboring H show very small ICOHP, which is consistent with the assumption that He does not form significant chemical bonds with neighboring atoms. The small but non-negligible ICOHP results for He and some of the neighboring atoms are caused by the projection of the crystal orbitals onto He atomic orbitals, which is a process that is largely depends on the choice of the sphere radius and may erroneously show a finite value.

Supplementary Table 5. The ICOHP of He and its neighbor atoms in $(H_2O)_2He$ under 400 and 500 GPa

	400 GPa		500 GPa	
	d(Å)	ICOHP(eV)	d(Å)	ICOHP(eV)
He-O	1.727	0.007	1.694	0.054
He-H1	1.386	0.434	1.348	0.116
He-H2	1.329	0.225	1.304	0.148

Supplementary Table 6. The ICOHP of He and its neighbor atoms in NH_3He under 400 and 500 GPa

	400 GPa		500 GPa	
	d(Å)	ICOHP(eV)	d(Å)	ICOHP(eV)
He-N	1.737	0.126	1.692	0.140
He-H1	1.429	0.053	1.388	0.010
He-H2	1.291	-0.061	1.267	-0.048
He-H3	1.336	-0.014	1.289	-0.024

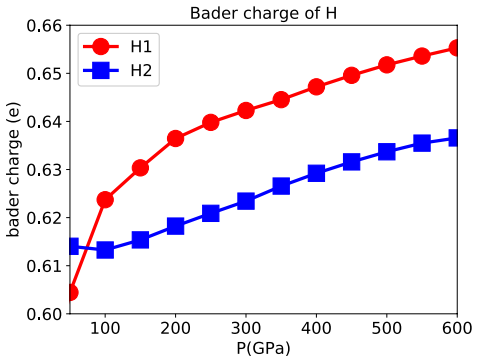

Supplementary Figure 2. The Bader valence charge on 2 H atoms occupying different equivalent positions.

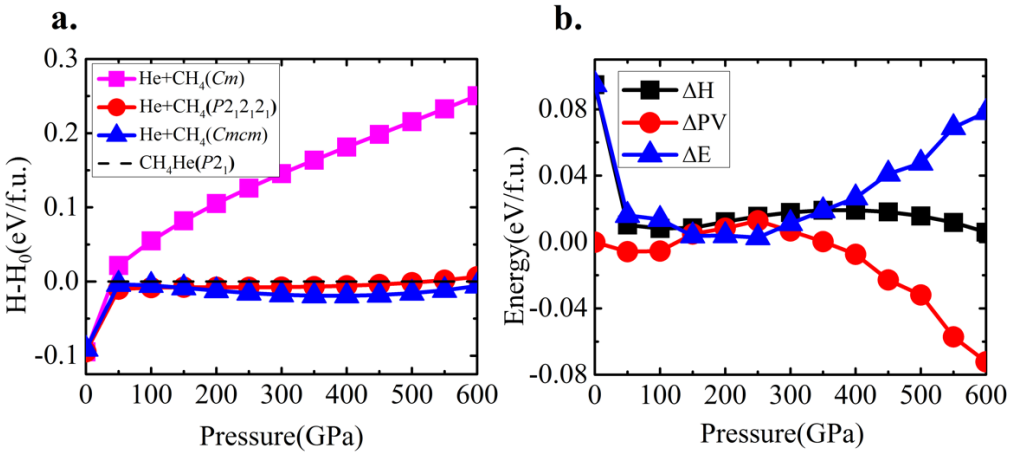

Supplementary Figure 3. Energies of CH_4+He system. (a) Relative enthalpy of CH_4+He. (b) The energies differences between CH_4He and its separate phase.

Supplementary Note 3

Here, we track inter- and intra- molecular H-O distance. The red solid line with circles is for inter-molecular H-O distance. The blue solid line with squares is for the intra-molecular H-O distance. In the case of $(H_2O)_2He$, we can see the inter-molecular H-O distance is larger than the intra-molecular distance. When pressure above 400 GPa, they become very close. In the case of compressed ice with the space group of $Cmc2_1$(shown Supplementary Fig. 4d), the inter- and intra- molecular distances become equal at around 150 GPa. The existence of He prevents the hydrogen-bond symmetrization in H_2O when the system is compressed.

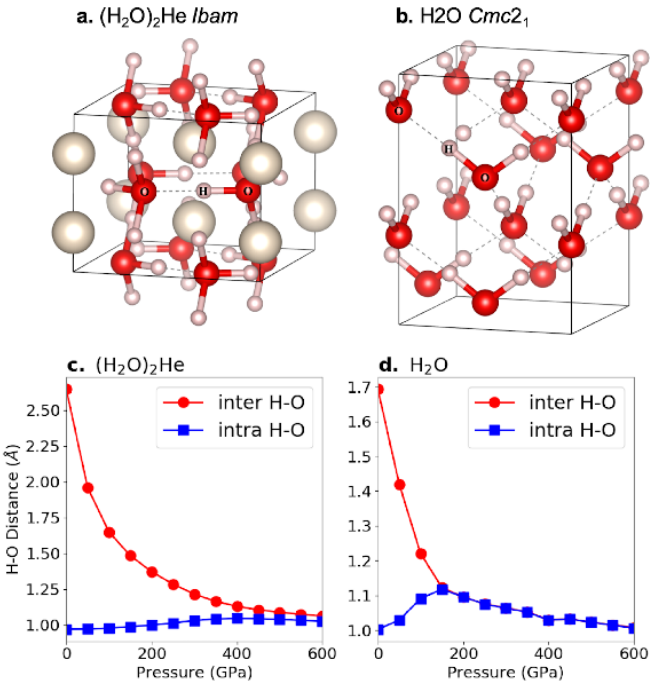

Supplementary Figure 4. H-O atomic distances. (a) The structure of $(H_2O)_2He$ in space group of *Ibam*. (c) The H_2O structure in space group of $Cmc2_1$. (b) and (d) the H-O distance in of inter- and intra-molecules in $(H_2O)_2He$ and H_2O.

Supplementary Note 4

The presence of the Hydrogen bonds complicates the energy landscape of the system and increases the difficulty of searching the global minimum point in the structure space. We therefore conducted a thorough structure search using an effective search algorithm. Under each pressure point, the conceived compositions are searched for 30 generations and sometimes have been redone for 1 or 2 times. Several (about 5-10) predicted structures are further studied and their energies are compared in order to identify the most stable structure. On the other hand, the complexity originated from hydrogen bonds are only important while the molecules remain, which is a structure feature that will also greatly reduce the structure search space. Furthermore, it is also true that the structure search is always limited by the size of the search unit, and a more stable structure cannot be completely excluded especially for a system with more complicated energy landscape. However, the energy improvement from the possible "missing" structures should be incremental. The structures obtained in the current work, even if they are not the most stable structure due to the limitation of the search unit, they should carry the correct chemistry and the conclusion about He insertion in each compound should not be altered.

For a molecular crystal under high pressure, the direction and length of hydrogen bonds are subject to large changes. Instead of counting the number of the hydrogen bonds, we calculate and show the change of the 1st and 2nd O-H distances as functions of pressure, with and without He insertion. H_2O will lose its molecular feature while the 1st and 2nd O-H distances become equal. Our results show that the insertion of He into H_2O actually prevents the ionization of H_2O crystal.

In Supplementary Fig. 5a, the solid line with circles are the function curve of 1st and 2nd order O-H distance in H_2O with a space group of $Cmc2_1$. The red line and blue line are the closest and 2nd close distance, respectively. The green and black lines with square symbols are respectively the closest and 2nd close distances of O-H in $(H_2O)_2He$. The H_2O units' self-ionization pressure is raised with the existence of He. In Supplementary Fig. 5b, the

interatomic O-O distance shows that, with the existence of He the O-O distance is smaller in $(H_2O)_2He$ than in the compressed ice, which indicates the reorientation of H_2O unit with the aid of He atom to reduce the volume when the system is compressed.

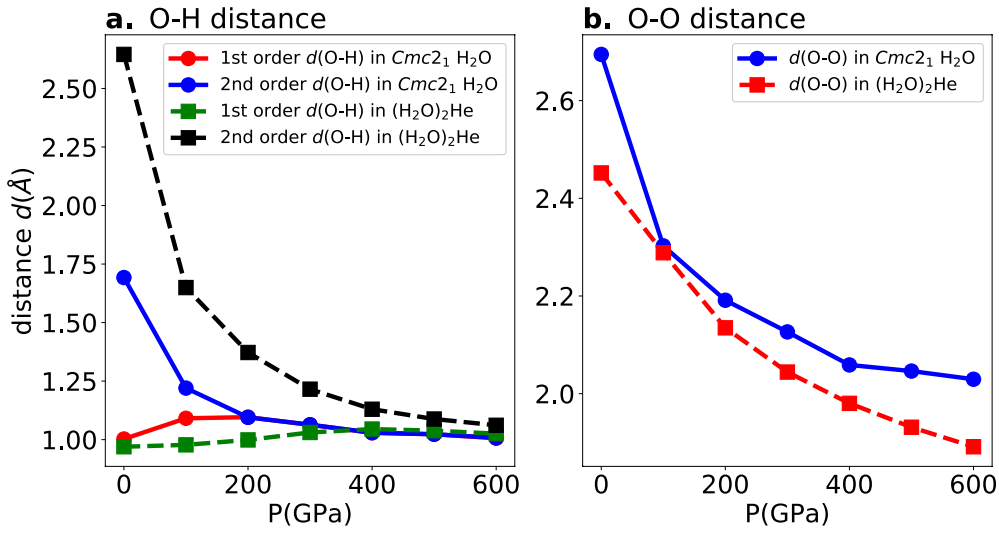

Supplementary Figure 5. O-H and O-O distances. (a) The closest and the 2nd close distances of O-H are shown as functions of pressure. (b) The O-O distance in H_2O and $(H_2O)_2He$.

Supplementary Note 5

We compare the PBE results for He insertion in H_2O with the calculations using Heyd-Scuseria-Ernzerhof hybrid functional (HSE06)[2] that is essentially the same as PBE0 as used in the paper of Griffith[3] et al. The only difference is that HSE06 cut the long-range exchange and replace it with a DFT only functional. We calculated the transition pressure for He insertion reaction with H_2O. Only the $Pn\bar{3}m$ structure was taken for pure H_2O. In the PBE calculation, $(H_2O)_2He$ gain the stability relative to $Pn\bar{3}m$ H_2O at 293 GPa, while this pressure becomes 324 GPa for HSE06. Therefore, the improvement of the exchange functional does not drastically change the transition pressure of the He insertion reaction with polar molecular crystals. We include this test result in the Supplementary Fig.6.

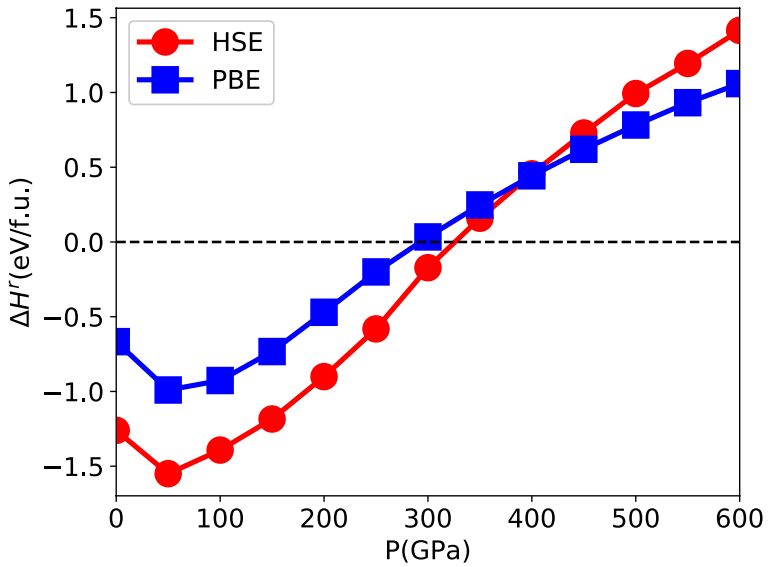

Supplementary Figure 6. The relative enthalpy sum of H_2O in space group of $Pn\bar{3}m$ and elemental He referred to $(H_2O)_2He$. The blue and red symbols show the results obtained by PBE and HSE functionals.

Supplementary Note 6

The PAW potentials have the capability to reconstruct the core and usually behave much better than traditional pseudopotentials under high pressure. However, it is a good idea to compare the equation of states (EOS) calculated by PAW potentials and a chosen full potential method. We therefore employed the LAPW method[4] as implemented in the ELK program (http://elk.sourceforge.net/) and calculated the EOS of NH_3He and $(H_2O)_2He$ and compared them with PAW potential results. In both full-potential and pseudopotential method, we track the internal energy change per atom for NH_3He and $(H_2O)_2He$ from 300 to 600 GPa. The results are shown in the figure below. The energy change per atom from 300 to 600 GPa agrees in both full-potential and pseudopotential method for both the cases of NH_3He and $(H_2O)_2He$. This proves the validity of using PAW potentials to study our systems up to 600 GPa.

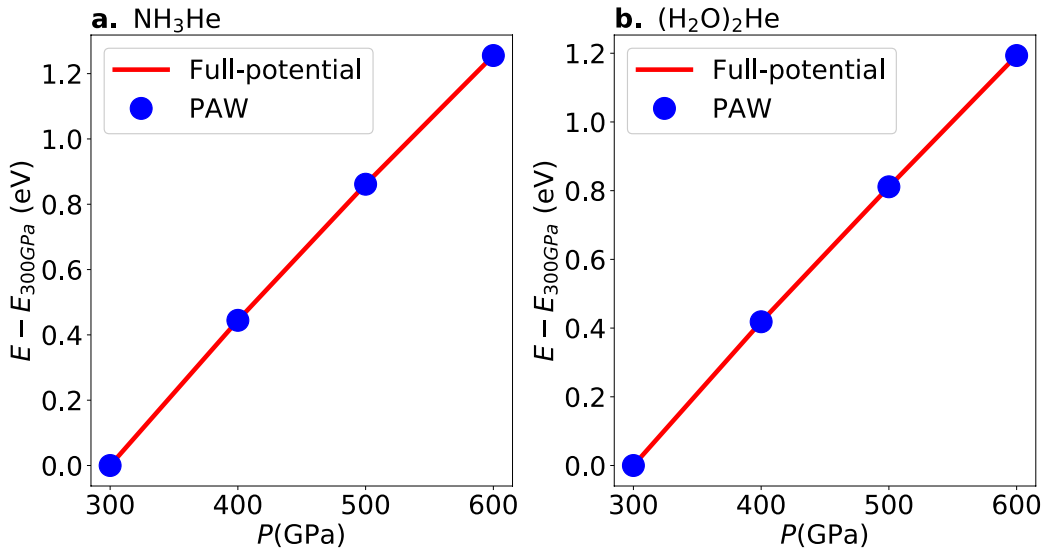

Supplementary Figure 7. The comparison of Equation of States for He inserted compounds. (a) NH_3He; (b) $(H_2O)_2He$.

Supplementary Table 7. Space groups and K-meshes for the structures of each studied compound. In our calculations, we use the Monkhorst-Pack mesh.

Compounds	Space group	MP K-mesh
NH_3	$P2_13$	$6 \times 6 \times 6$
	$P2_12_12_1$	$8 \times 6 \times 4$
	$Pma2$	$6 \times 8 \times 4$
	$P2_1/m$	$8 \times 6 \times 4$
	$Pnma$	$4 \times 6 \times 8$
NH_3	$P2_12_12_1$	$6 \times 8 \times 4$
H_2O	$Cmc2_1$	$6 \times 4 \times 4$
	$Pn\bar{3}m$	$12 \times 12 \times 12$
	$Pbcm$	$12 \times 8 \times 10$
$(H_2O)_2He$	$Ibam$	$4 \times 6 \times 8$

Supplementary Note 7

We tested the effect of the dispersion forces by using the D2 method of Grimme[5] in the calculations. The results are shown in the following figure. Comparing these results with Figure 1 in the main text, we conclude that the inclusion of the dispersion forces have negligible effect. The insertion of He in the molecular crystals does not cause significant change to the dispersion interactions among the molecules.

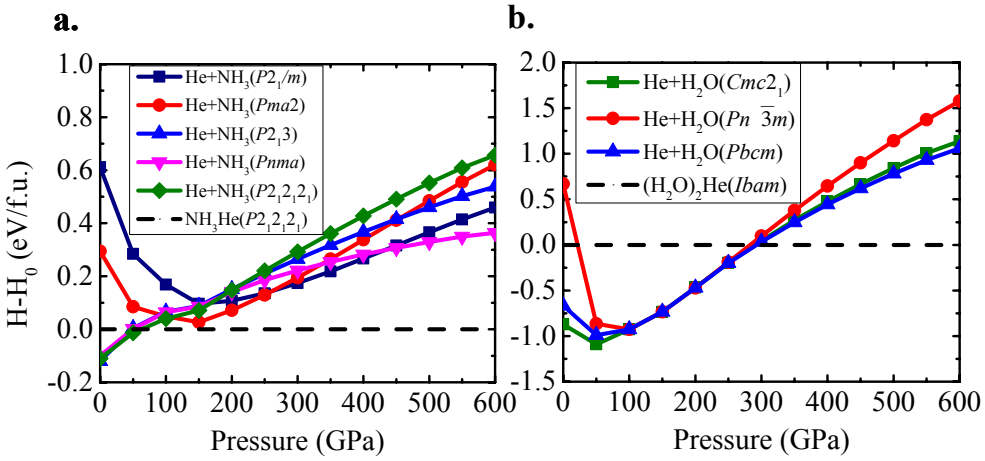

Supplementary Figure 8. The calculated reaction enthalpy of He insertion when the van der Waals interaction is taken into consideration. (a) ammonia and (b) ice.

Supplementary Note 8

Zero-point energy (ZPE) is important for systems containing H atoms. We tested its effects using frozen phonon method[6]. Comparing them with Figure 1 in the main text, we conclude that the inclusion of ZPE only make slight changes to the He insertion reaction. The transition pressure changes from 45 GPa to 36 GPa for NH_3 and from 300 GPa to 328 GPa for H_2O. This is due to the fact that the inclusion of He does not change much of the bonding strength of H with N or O atoms and the ZPE are eventually cancelled between the molecular crystals with and without He insertion. The Helium's contribution to the ZPE also cancelled because of the same reason.

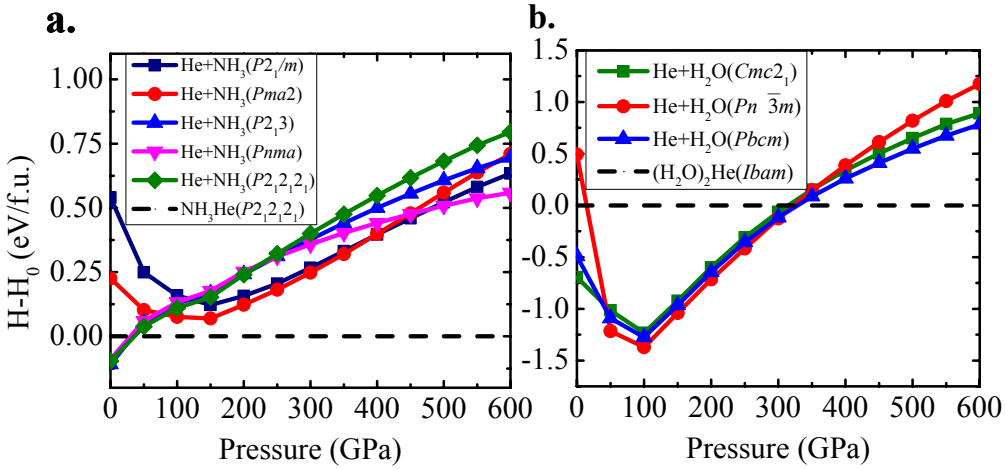

Supplementary Figure 9. The calculated reaction enthalpy of He insertion including the zero-point energies. (a) ammonia and (b) ice.

Supplementary References

1 Dronskowski, R. & Bloechl, P. E. Crystal orbital Hamilton populations (COHP): energy-resolved visualization of chemical bonding in solids based on density-functional calculations. *J. Phys. Chem.* **97**, 8617-8624, (1993).

2 Heyd, J., Scuseria, G. E. & Ernzerhof, M. Hybrid functionals based on a screened Coulomb potential. *J. Chem. Phys.* **118**, 8207-8215, (2003).

3 Griffiths, G. I. G., Misquitta, A. J., Fortes, A. D., Pickard, C. J. & Needs, R. J. High pressure ionic and molecular crystals of ammonia monohydrate within density functional theory. *J. Chem. Phys.* **137**, 9, (2012).

4 Blaha, P., Schwarz, K., Sorantin, P. & Trickey, S. B. Full-potential, linearized augmented plane-wave programs for crystalline systems. *Comput. Phys. Commun.* **59**, 399-415, (1990).

5 Grimme, S. Semiempirical GGA-type density functional constructed with a long-range dispersion correction. *J. Comput. Chem.* **27**, 1787–1799, (2006).

6 Gonze, X. Adiabatic density-functional perturbation theory. *Phys. Rev. A* **52**, 1096-1114, (1995).